4-1-2022

The effect of scan and patient parameters on the diagnostic performance of AI for detecting coronary stenosis on coronary CT angiography

Rebecca Jonas
Thomas Jefferson University

Emil Barkovich
The George Washington University School of Medicine

Andrew D Choi
The George Washington University School of Medicine

William F Griffin
The George Washington University School of Medicine

Joanna Riess
The George Washington University School of Medicine

See next page for additional authors

Recommended Citation
Jonas, Rebecca; Barkovich, Emil; Choi, Andrew D; Griffin, William F; Riess, Joanna; Marques, Hugo; Chang, Hyuk-Jae; Choi, Jung Hyun; Doh, Joon-Hyung; Her, Ae-Young; Koo, Bon-Kwon; Nam, Chang-Wook; Park, Hyung-Bok; Shin, Sang-Hoon; Cole, Jason; Gimelli, Alessia; Khan, Muhammad Akram; Lu, Bin; Gao, Yang; Nabi, Faisal; Nakazato, Ryo; Schoepf, U Joseph; Driessen, Roel S; Bom, Michiel J; Thompson, Randall C; Jang, James J; Ridner, Michael; Rowan, Chris; Avelar, Erick; Généreux, Philippe; Knaapen, Paul; de Waard, Guus A; Pontone, Gianluca; Andreini, Daniele; Guglielmo, Marco; Al-Mallah, Mouaz H; Jennings, Robert S; Crabtree, Tami R; and Earls, James P, "The effect of scan and patient parameters on the diagnostic performance of AI for detecting coronary stenosis on coronary CT angiography" (2022). *Division of Internal Medicine Faculty Papers & Presentations.* Paper 47.
https://jdc.jefferson.edu/internalfp/47

Authors

Rebecca Jonas, Emil Barkovich, Andrew D Choi, William F Griffin, Joanna Riess, Hugo Marques, Hyuk-Jae Chang, Jung Hyun Choi, Joon-Hyung Doh, Ae-Young Her, Bon-Kwon Koo, Chang-Wook Nam, Hyung-Bok Park, Sang-Hoon Shin, Jason Cole, Alessia Gimelli, Muhammad Akram Khan, Bin Lu, Yang Gao, Faisal Nabi, Ryo Nakazato, U Joseph Schoepf, Roel S Driessen, Michiel J Bom, Randall C Thompson, James J Jang, Michael Ridner, Chris Rowan, Erick Avelar, Philippe Généreux, Paul Knaapen, Guus A de Waard, Gianluca Pontone, Daniele Andreini, Marco Guglielmo, Mouaz H Al-Mallah, Robert S Jennings, Tami R Crabtree, and James P Earls

Clinical Imaging 84 (2022) 149–158

Contents lists available at ScienceDirect

Clinical Imaging

journal homepage: www.elsevier.com/locate/clinimag

Cardiothoracic Imaging

The effect of scan and patient parameters on the diagnostic performance of AI for detecting coronary stenosis on coronary CT angiography

Rebecca A. Jonas [a], Emil Barkovich [b], Andrew D. Choi [b], William F. Griffin [b], Joanna Riess [b], Hugo Marques [c], Hyuk-Jae Chang [d], Jung Hyun Choi [e], Joon-Hyung Doh [f], Ae-Young Her [g], Bon-Kwon Koo [h], Chang-Wook Nam [i], Hyung-Bok Park [j], Sang-Hoon Shin [k], Jason Cole [l], Alessia Gimelli [m], Muhammad Akram Khan [n], Bin Lu [o], Yang Gao [o], Faisal Nabi [p], Ryo Nakazato [q], U. Joseph Schoepf [r], Roel S. Driessen [s], Michiel J. Bom [s], Randall C. Thompson [t], James J. Jang [u], Michael Ridner [v], Chris Rowan [w], Erick Avelar [x], Philippe Généreux [y], Paul Knaapen [s], Guus A. de Waard [s], Gianluca Pontone [z], Daniele Andreini [z], Marco Guglielmo [z], Mouaz H. Al-Mallah [p], Robert S. Jennings [aa], Tami R. Crabtree [aa], James P. Earls [aa,b,*]

[a] Department of Internal Medicine, Thomas Jefferson University Medical Center, Philadelphia, PA, USA
[b] Department of Radiology and Division of Cardiology, The George Washington University School of Medicine, Washington, DC, USA
[c] Nova Medical School - Faculdade de Ciências Médicas, Lisboa, Portugal
[d] Division of Cardiology, Severance Cardiovascular Hospital and Severance Biomedical Science Institute, Yonsei University College of Medicine, Yonsei University Health System, Seoul, South Korea
[e] Ontact Health, Inc., Seoul, South Korea
[f] Division of Cardiology, Inje University Ilsan Paik Hospital, South Korea
[g] Kang Won National University Hospital, Chuncheon, South Korea
[h] Department of Internal Medicine, Seoul National University Hospital, Seoul, South Korea
[i] Cardiovascular Center, Keimyung University Dongsan Hospital, Daegu, South Korea
[j] Division of Cardiology, Department of Internal Medicine, International St. Mary's Hospital, Catholic Kwandong University College of Medicine, Incheon, South Korea
[k] National Health Insurance Service Ilsan Hospital, Goyang, South Korea
[l] Mobile Cardiology Associates, Mobile, AL, USA
[m] Department of Imaging, Fondazione Toscana Gabriele Monasterio, Pisa, Italy
[n] Cardiac Center of Texas, McKinney, TX, USA
[o] State Key Laboratory of Cardiovascular Disease, Fuwai Hospital, Beijing, China
[p] Houston Methodist Hospital, Houston, TX, USA
[q] Cardiovascular Center, St. Luke's International Hospital, Tokyo, Japan
[r] Medical University of South Carolina, Charleston, SC, USA
[s] Amsterdam University Medical Center, VU University Medical Center, Amsterdam, the Netherlands
[t] St. Luke's Mid America Heart Institute, Kansas City, MO, USA
[u] Kaiser Permanente San Jose Medical Center, San Jose, CA, USA
[v] Heart Center Research, LLC, Huntsville, AL, USA
[w] Renown Heart and Vascular Institute, Reno, NV, USA
[x] Oconee Heart and Vascular Center at St Mary's Hospital, Athens, GA, USA
[y] Gagnon Cardiovascular Institute at Morristown Medical Center, Morristown, NJ, USA
[z] Centro Cardiologico Monzino, IRCCS, Milan, Italy
[aa] Cleerly Inc, New York, NY, USA

ARTICLE INFO

ABSTRACT

Abbreviations: AI, Artificial Intelligence; AI-QCT, Artificial Intelligence Enabled Quantitative Coronary Computed Tomographic Angiography; CAD, Coronary Artery Disease; CAD-RADS, Coronary Artery Disease Reporting and Data System; CCTA, Coronary computed tomography angiography; DS, Dual source; FBP, Filtered Back Projection; FDA, Food and Drug Administration; FFR, Fractional Flow Reserve; IR, Iterative Reconstruction; LAD, Left Anterior Descending; LCx, Left Circumflex; LM, Left Main; MDCT, Multidetector Computed Tomography; PDA, Posterior Descending Artery; QCA, quantitative coronary angiography; RCA, Right Coronary Artery; SS, Single source.

* Corresponding author at: MD FSSCYT George Washington University School of Medicine Washington DC.
E-mail address: jearls@mfa.gwu.edu (J.P. Earls).

https://doi.org/10.1016/j.clinimag.2022.01.016
Received 5 October 2021; Received in revised form 21 January 2022; Accepted 24 January 2022
Available online 3 February 2022

Keywords:
Coronary computed tomography angiography
CCTA
Coronary artery disease
Atherosclerosis
Artificial intelligence
Image quality

Objectives: To determine whether coronary computed tomography angiography (CCTA) scanning, scan preparation, contrast, and patient based parameters influence the diagnostic performance of an artificial intelligence (AI) based analysis software for identifying coronary lesions with ≥50% stenosis.

Background: CCTA is a noninvasive imaging modality that provides diagnostic and prognostic benefit to patients with coronary artery disease (CAD). The use of AI enabled quantitative CCTA (AI-QCT) analysis software enhances our diagnostic and prognostic ability, however, it is currently unclear whether software performance is influenced by CCTA scanning parameters.

Methods: CCTA and quantitative coronary CT (QCT) data from 303 stable patients (64 ± 10 years, 71% male) from the derivation arm of the CREDENCE Trial were retrospectively analyzed using an FDA-cleared cloud-based software that performs AI-enabled coronary segmentation, lumen and vessel wall determination, plaque quantification and characterization, and stenosis determination. The algorithm's diagnostic performance measures (sensitivity, specificity, and accuracy) for detecting coronary lesions of ≥50% stenosis were determined based on concordance with QCA measurements and subsequently compared across scanning parameters (including scanner vendor, model, single vs dual source, tube voltage, dose length product, gating technique, timing method), scan preparation technique (use of beta blocker, use and dose of nitroglycerin), contrast administration parameters (contrast type, infusion rate, iodine concentration, contrast volume) and patient parameters (heart rate and BMI).

Results: Within the patient cohort, 13% demonstrated ≥50% stenosis in 3 vessel territories, 21% in 2 vessel territories, 35% in 1 vessel territory while 32% had <50% stenosis in all vessel territories evaluated by QCA. Average AI analysis time was 10.3 ± 2.7 min. On a per vessel basis, there were significant differences only in sensitivity for ≥50% stenosis based on contrast type (iso-osmolar 70.0% vs non isoosmolar 92.1% $p = 0.0345$) and iodine concentration (<350 mg/ml 70.0%, 350-369 mg/ml 90.0%, 370–400 mg/ml 90.0%, >400 mg/ml 95.2%; $p = 0.0287$) in the context of low injection flow rates. On a per patient basis there were no significant differences in AI diagnostic performance measures across all measured scanner, scan technique, patient preparation, contrast, and individual patient parameters.

Conclusion: The diagnostic performance of AI-QCT analysis software for detecting moderate to high grade stenosis are unaffected by commonly used CCTA scanning parameters and across a range of common scanning, scanner, contrast and patient variables.

Condensed abstract: An AI-enabled quantitative CCTA (AI-QCT) analysis software has been validated as an effective tool for the identification, quantification and characterization of coronary plaque and stenosis through comparison to blinded expert readers and quantitative coronary angiography. However, it is unclear whether CCTA screening parameters related to scanner parameters, scan technique, contrast volume and rate, radiation dose, or a patient's BMI or heart rate at time of scan affect the software's diagnostic measures for detection of moderate to high grade stenosis. AI performance measures were unaffected across a broad range of commonly encountered scanner, patient preparation, scan technique, intravenous contrast and patient parameters.

1. Background

Coronary computed tomography angiography (CCTA) has established itself as an effective tool for diagnosing and grading coronary artery disease (CAD) severity through high performance against the current gold standard, invasive coronary angiography (ICA).[1,2] Furthermore, data derived through CCTA improves clinical care by guiding disease prognostication, reducing unnecessary invasive testing and improving overall outcomes.[3–6] While these scans provide data that have direct clinical utility, they also provide a quantity of data that qualitative reads by human readers cannot generate in a clinically useful period of time.

The use of artificial intelligence (AI) for image analysis and interpretation has further enhanced our diagnostic and prognostic capability by using pixel level analytics and automated learning algorithms for rapid adaptation.[7–9] Given AI guided CCTA's (AI-QCT's) consistency, expediency and high performance for stenosis grading against gold standards like expert readers, quantitative invasive coronary angiography (QCA) and fractional flow reserve (FFR), CCTA analysis is likely to employ AI on a widespread basis in the future.[10,11] While AI-QCT may have the capability to rapidly and accurately analyze CCTA images, widespread use will require an understanding of its performance across the various parameter settings. At this early stage, it is not yet clear whether AI-QCT's performance changes across common scanning parameters. However, if AI-QCT performance is comparable to QCA for plaque analysis without limitation across scan parameters, this would support the widespread use of a safe, noninvasive mode of mild to moderate lesion diagnosis and further AI-QCT generated atherosclerosis analyses on a grand scale.

This study evaluated the sensitivity, specificity and accuracy of AI-QCT analysis compared to QCA for identifying moderate to high grade stenosis (≥50% stenosis) across a range of commonly encountered scanner, patient preparation, scan technique, intravenous contrast and patient parameters.

2. Methods

2.1. Subjects

We retrospectively evaluated data from 303 patients including CCTA, FFR and QCA from the derivation arm of the Computed TomogRaphic Evaluation of Atherosclerotic Determinants of Myocardial IsChEmia (CREDENCE) Trial.[12,13] The CREDENCE trial (clinicaltrials.gov NCT02173275) was a prospective, multicenter diagnostic derivation-validation, controlled clinical trial recruiting patients from 2014 to 2017.[12,13] Sites and Investigators are listed in Appendix B. All enrolled CREDENCE subjects underwent CCTA, and QCA with FFR. The IRB of each site approved the study protocol and patients provided written informed consent. Inclusion and exclusion criteria and clinical sites are listed in the supplement (Appendix A). This study is an investigator-initiated study. Cleerly Inc. had no role in study design or performance. Cleerly Inc. performed the CCTA analyses for the study in a blinded manner and provided statistical services as determined and requested by the study investigators.

2.2. CT imaging protocols

CCTA was performed using a CT scanner with ≥64-detector rows. Sites were instructed to perform CCTA in accordance with guidelines from the Society of Cardiovascular Computed Tomography (SCCT).[12,14]

2.3. CCTA scanning parameters

The software's sensitivity, specificity and accuracy for detecting coronary lesions ≥50% stenosis were tested across a multitude of screening parameters including scanner vendor (GE, Philips, Siemens, Toshiba), scanner model, single vs. dual source scanning, gating technique (prospective vs. retrospective helical), bolus type (tracker vs. test bolus) and injection rate, contrast agent (Iodixanol [Visipaque] vs. all others), contrast volume and iodine concentration, radiation parameters including tube voltage and dose length product, mode of image generation (filter back projection vs. iterative reconstruction), administration of beta blockers or nitroglycerine prior to scanning, and patient's average heart rate and BMI at time of scan. The AI-software's diagnostic performance measures were determined based on concordance with QCA measurements and subsequently compared across screening parameters.

2.4. Quantitative coronary angiography

Invasive coronary angiography was performed in agreement with clinical indications and imaging standards. A dedicated core laboratory performed blinded QCA in two orthogonal views on a per lesion basis of every lesion visually ≥30% diameter stenosis in vessels with a reference vessel diameter ≥2.0 mm. Lesions estimated to be less than 30% were recorded as no stenosis.

2.5. Artificial intelligence-based segmentation and stenosis quantification

The AI-based approach to CCTA interpretation in this study was performed using an FDA-cleared software service (Cleerly Lab, Cleerly, New York, NY) that performs automated analysis of CCTA using a series of validated convolutional neural network models (including VGG19 network, 3D U-Net, and VGG Network Variant) for image quality assessment, coronary segmentation and labeling, lumen wall evaluation and vessel contour determination (Fig. 1) and plaque characterization.[15] Training and testing were performed on a proprietary database. A centerline algorithm was developed from 1,007,945 images, which incorporated 23,068 vessels from 3671 patients. Lumen and vessel wall algorithms were developed from 1,414,877 images, comprised of 8555 vessels from 3676 patients. First, the AI-aided approach produces a centerline along each coronary artery for lumen and outer vessel wall contouring. This is applied to each phase of the examination. The two optimal series are then identified for further analysis. These top two phases are evaluated interactively on a per vessel basis, e.g., the right

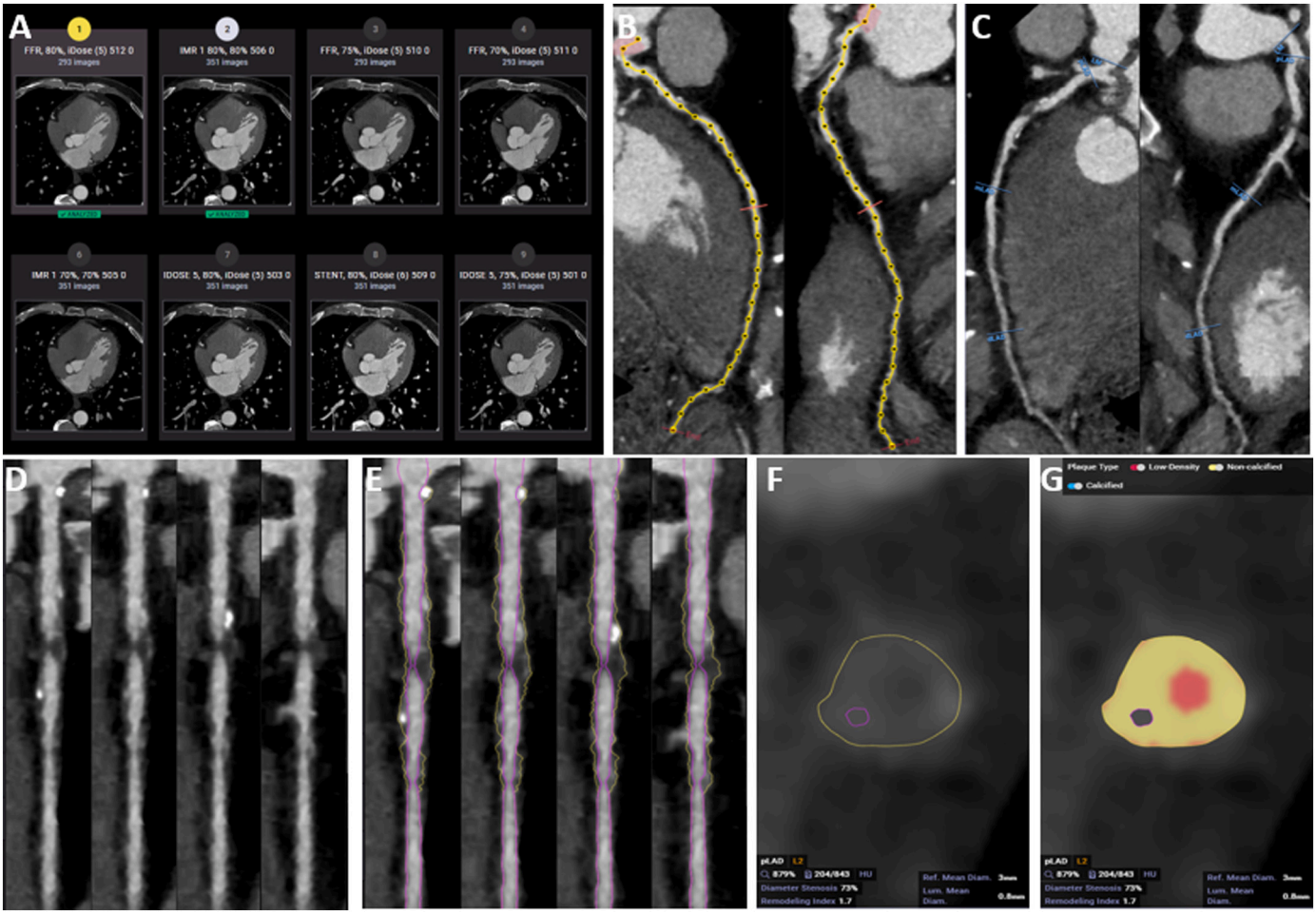

Fig. 1. A stepwise explanation of how AI-QCT calculates % diameter stenosis. AI-QCT segmentation and analysis of a CCTA from a 53 yr old male with chest pain and a positive nuclear stress test. A. Initially, all available series are evaluated by two machine learned algorithms to select the two series with optimal image quality for further analysis. B. A centerline algorithm is performed along each coronary artery. C. Once coronary artery segmentation is performed, an automated labeling (blue line and boxes) is done to classify arteries by their location as well the proximal, mid and distal portions within a single vessel. D and E. The lumen (purple) and outer vessel wall (yellow) contouring boundaries are determined. F. For each plaque, the cross-sectional slice that demonstrates the greatest absolute narrowing, % diameter stenosis severity and remodeling index is automatically calculated (73% proximal LAD stenosis with a RI of 1.7 depicted). G. A color overlay is performed based upon HU attenuation, in this case a predominantly noncalcified plaque is present with a low-density non-calcified core (red overlay). (For interpretation of the references to color in this figure legend, the reader is referred to the web version of this article.)

coronary artery (RCA) will be reconstructed from the phase which yields the highest RCA image quality, while the posterior descending artery (PDA) may come from the second phase if the PDA has a higher image quality on that phase.

Once coronary artery segmentation is performed, segments are labeled in an automated fashion to classify the segment by vessel, and whether it is in the proximal, mid or distal portion of that vessel. For stenosis evaluation the software places markers at the beginning and end of each lesion and selects the mean coronary diameter at the closest normal proximal reference cross section as the reference diameter (D_{ref}), and the mean diameter on the cross section demonstrating the greatest absolute stenosis (D_s). The % diameter stenosis is then automatically calculated using the following formula: % Diameter stenosis = $(1 - (D_s/D_{ref})) \times 100$. After the AI algorithm has finished all operations, as mandated by the FDA, a quality control cardiac CT trained technician reviews the results and makes manual adjustments if necessary. AI computational analysis time was 10.3 ± 2.7 min.

2.6. Stenosis comparison QCA vs CCTA

QCA stenosis was measured by core lab readers in each vessel territory. If QCA detected stenosis, AI-based stenosis evaluation was then conducted on those coronary segments using an SCCT 18-segment coronary tree model. When QCA evaluated a vessel territory and recorded 0% stenosis, that value was applied to each segment in the territory. However, if QCA was present in only one segment of the territory, and identified stenoses, values were treated as missing in the other segments. Thus, the denominator for per-segment analysis equals the sum of all segments in all territories where QCA is 0% and all segments where QCA was measured and recorded as >0%. The maximum QCA and AI-based diameter stenosis were calculated across segments for each stenotic vessel. Where QCA was measured in just one segment in the vessel, that value was applied to the vessel. Per-vessel territory and per-patient results were obtained in a similar manner. No cases were excluded due to impaired image quality on CCTA. If impaired image quality was present due to motion, beam hardening or other artifact, just the portion of the coronary artery with poor quality was excluded from the analysis. Any quantitative data from the excluded segment is not included in the final report.

2.7. Statistical analysis

Analysis was performed using SAS software version 9.4 (SAS Inc., Cary, NC). The diagnostic performance of AI-based diameter stenosis was evaluated by calculating the sensitivity, specificity and diagnostic accuracy for identifying ≥50% stenosis on a segment, vessel, vessel territory and patient basis using QCA as the reference standard. Area under the receiver operating characteristic curves was used to evaluate the diagnostic performance for ≥50% stenosis per QCA. The comparability of the continuous measures of diameter stenosis for AI and QCA were assessed via correlation using Pearson's correlation coefficients and calculation of the mean difference (bias). Sensitivity, specificity, and diagnostic performance for ≥50% diameter stenosis per vessel territory were compared across patient subgroups using logistic generalized estimating equation (GEE) regression models, to account for the potential correlation of multiple vessel territories per patient.

AI diagnostic performance on a per patient basis was compared across categorical scan parameters using the Chi-square or Fisher's exact test. Ordered parameters were compared using the Jonckheere-Terpstra test. Diagnostic performance measures for vessel territories were compared across scan parameters using a logistic generalized estimating equation model to account for any within subject correlation of the three vessel territories measured per subject.

3. Results

3.1. Study population

Baseline characteristics of the study population are listed in Table 1. A total of 303 of the 307 (98%) subjects comprising the derivation arm of the CREDENCE cohort[12,13] were included; 4 patients were excluded due to corruption of their CT imaging data. Of the 303 patients evaluated, 175 (57.8%) had obstructive disease while 128 (42.2%) had non-obstructive disease.

3.2. AI analysis success

The AI algorithm was run successfully in all 303 patients (100%). There was a total of 171,195 mm of vessel length evaluated in the entire cohort, of this, a total of 1861 mm (1.09%) was excluded due to impaired image quality. The length of an exclusion averaged 14.1 (± 13.9) mm and were longer in the RCA (15.22 ± 6.72 mm) than the LAD (7.62 ± 4.12 mm) or the Circumflex (7.58 ± 8.13 mm) arteries.

3.3. AI diagnostic measurements by scanning parameters at the patient level

AI sensitivity, specificity, and accuracy measurements for detecting moderate stenosis at the patient level are listed for each of the tested scanning parameters in Table 2. The table reflects that at the patient level, there were no significant differences in AI diagnostic measurements based on scanner type (vendor, model, single vs. dual source), gating technique, bolus type, contrast features (agent, volume, iodine concentration), radiation features (tube voltage, dose length product), image generation (filtered back projection vs. iterative reconstruction),

Table 1
Patient characteristics.

Patient parameters	
Age	64 ± 10
Male	71% (218)
BMI	26 ± 4
Race	
Black	2% (7)
Asian	71% (217)
White	27% (82)
Hypertension	64% (197)
Hyperlipidemia	44% (136)
Diabetes	31% (95)
Current Smoker	17% (53)
Prior Smoker	34% (103)
# Diseased Vessel Territories (≥50% CCTA stenosis)	
0	32% (96)
1	35% (105)
2	21% (64)
3	13% (38)

Scan parameters	
Scanner vendor	
General Electric	18% (54)
Philips	2% (5)
Siemens	43% (132)
Toshiba	38% (116)
Tube Voltage	
70 kV	0.3% (1)
80 kV	6% (17)
100 kV	38% (116)
120 kV	52% (160)
Other	4% (11)
Gating technique	
Prospective/sequential	31% (95)
Retrospective helical	61% (188)
Single beat acquisition	8% (23)

Table 2
AI Diagnostic performance by scanning parameter on the patient level.

Subgroup	Sensitivity	Specificity	Accuracy
Scanner vendor			
GE	96% (24/25)	82.8% (24/29)	89.9% (48/54)
Philips	100% (3/3)	50% (1/2)	80.0% (4/5)
Siemens	94.7% (71/75)	60% (33/55)	80.0% (104/130)
Toshiba	93.2% (69/74)	70% (28/40)	85.1% (97/114)
	0.9227	0.1312	0.4194
Scanner model			
Toshiba – Aquilion One	93.2% (69/74)	70.0% (28/40)	85.1% (97/114)
GE-VCT Light Speed 64	96.0% (24/25)	84.0% (21/25)	90.0% (45/50)
Siemens Dual Source Definition	100% (25/25)	58.3% (14/24)	76.6% (39/49)
All others	92.5% (49/53)	62.2% (23/37)	80% (72/90)
	0.7029	0.2001	0.3787
Single source vs dual source			
SS	93.8% (137/146)	71.3% (67/94)	85% (204/240)
DS	96.8% (30/31)	59.4% (19/32)	77.8% (49/63)
	>0.999	0.2116	0.1693
Average heart rate during CT			
≤70 bpm	94.6% (139/147)	69.0% (69/100)	84.2% (208/247)
>70 bpm	95.2% (20/21)	68.8% (11/16)	83.8% (31/37)
	>0.999	>0.999	0.9471
≤75 bpm	94.9% (149/157)	69.4% (75/108)	84.5% (224/265)
>75 bpm	90.9% (10/11)	62.5% (5/8)	79.0% (15/19)
	0.4648	0.7020	0.5165
≤70	94.6% (139/147)	69.0% (69/100)	84.2% (208/247)
71–80	100% (16/16)	69.2% (9/13)	86.2% (25/29)
>80	80.0% (4/5)	66.7% (2/3)	75.0% (6/8)
	0.9755	0.9801	0.9123
Beta blocker IV			
Yes	94.0% (141/150)	67.3% (76/113)	82.5% (217/263)
No	96.3% (26/27)	76.9% (10/13)	90.0% (36/40)
	>0.999	0.4783	0.2344
Nitroglycerin dose			
None	95.9% (47/49)	65.9% (29/44)	81.7% (76/93)
Low (0.1–0.4 mg)	95.2% (40/42)	65.7% (23/35)	81.8% (63/77)
High (>0.4 mg)	93.0% (80/86)	72.3% (34/47)	85.7% (114/133)
	0.4569	0.5054	0.3941
None	95.9% (47/49)	65.9% (29/44)	81.7% (76/93)
Some	93.8% (120/128)	69.5% (57/82)	84.3% (177/210)
	0.7287	0.6787	0.5790
Bolus tracker or test bolus			
BT	95.3% (101/106)	67.2% (43/64)	84.7% (144,185)
TB	93.0% (66/71)	70.5% (43/61)	82.6% (109/132)
	0.5249	0.6902	0.6185
Gating technique			
Prospective/sequential/ Single Beat	91.9% (68/74)	72.1% (31/43)	84.6% (99/117)
Retrospective helical	96.1% (99/103)	67.1% (55/82)	83.2% (154/185)
	0.3240	0.6853	0.7527
Contrast agent			
Visipaque	100% (5/5)	77.8% (7/9)	85.7% (12/14)
All others	94.2% (162/172)	67.5% (79/117)	83.4% (241/289)
	>0.999	0.7179	>0.999
Concentration mg iodine per mL			
Q1: <350	100% (5/5)	80.0% (8/10)	86.7% (13/15)
Q2: 350–369	94.1% (32/34)	70.3% (26/37)	81.7% (58/71)
Q3: 370–400	90.8% (59/65)	65.2% (30/46)	80.2% (89/111)
Q4: >400	97.3% (71/73)	68.8% (22/32)	88.6% (93.105)
	0.3731	0.5912	0.2411
Contrast injection rate (*cc/sec*)			
<5	89.5% (34/38)	66.7% (20/30)	79.4% (54/68)
5	95.3% (102/107)	72.7% (56/77)	85.9% (158/184)
>5	96.9% (31/32)	52.9% (9/17)	81.6% (40/49)
	0.1659	0.5554	0.6059
Contrast volume- *mg/kg body weight*			
Q1: <333.4	89.5% (34/38)	71.1% (27/38)	80.3% (61/76)
Q2: 333.4–408.2	93.3% (42/45)	63.3% (19/30)	81.3% (61/75)
Q3: 408.3–504.5	98.0% (49/50)	68.0% (17/25)	88.0% (66/75)
Q4: >504.5	95.5% (42/44)	71.9% (23/32)	85.5% (65/76)
	0.1688	0.9100	0.2378
Tube voltage			
≤80 kV	100% (8/8)	100% (10/10)	100% (18/18)
100 kV	91.8% (67/73)	60.0% (24/40)	80.5% (91/113)
120 kV	95.4% (83/87)	70.8% (51/72)	84.3% (134/159)
	0.5689	0.8529	0.8520
Dose length product (*mGy*cm*)			
Q1: <200.5	91.3% (42/46)	64.3% (18/28)	81.1% (60/74)
Q2: 200.5–365	95.2% (40/42)	71.9% (23/32)	85.1% (63/74)
Q3: 366–600.2	98.0% (42/43)	71.0% (22/31)	86.5% (64/74)
Q4: >600.2	93.2% (41/44)	68.8% (22/32)	82.9% (63/76)
	0.5930	0.7709	0.7296
BMI			
<30	94.4% (151/160)	69.6% (71/102)	84.7% (222/262)
≥30	94.1% (16/17)	62.5% (15/24)	75.6% (31/41)
	>0.999	0.5009	0.1434
Iterative reconstruction			
FBP	96.0% (24/25)	84.0% (21/25)	90.0% (45/50)
IR	94.1% (143/152)	64.4% (65/101)	82.2% (208/253)
Scanner vendor	>0.999	0.0589	0.1753

medication administration prior to imaging (beta blockade, nitroglycerine) or clinical (Figs. 2,3) patient features at time of scan (heart rate, BMI). While the p values for specificity of scanner vendor and scanner model were 0.13 and 0.2, respectively, these values are low suggesting a trend, but do not meet statistical significance ($P < 0.05$).

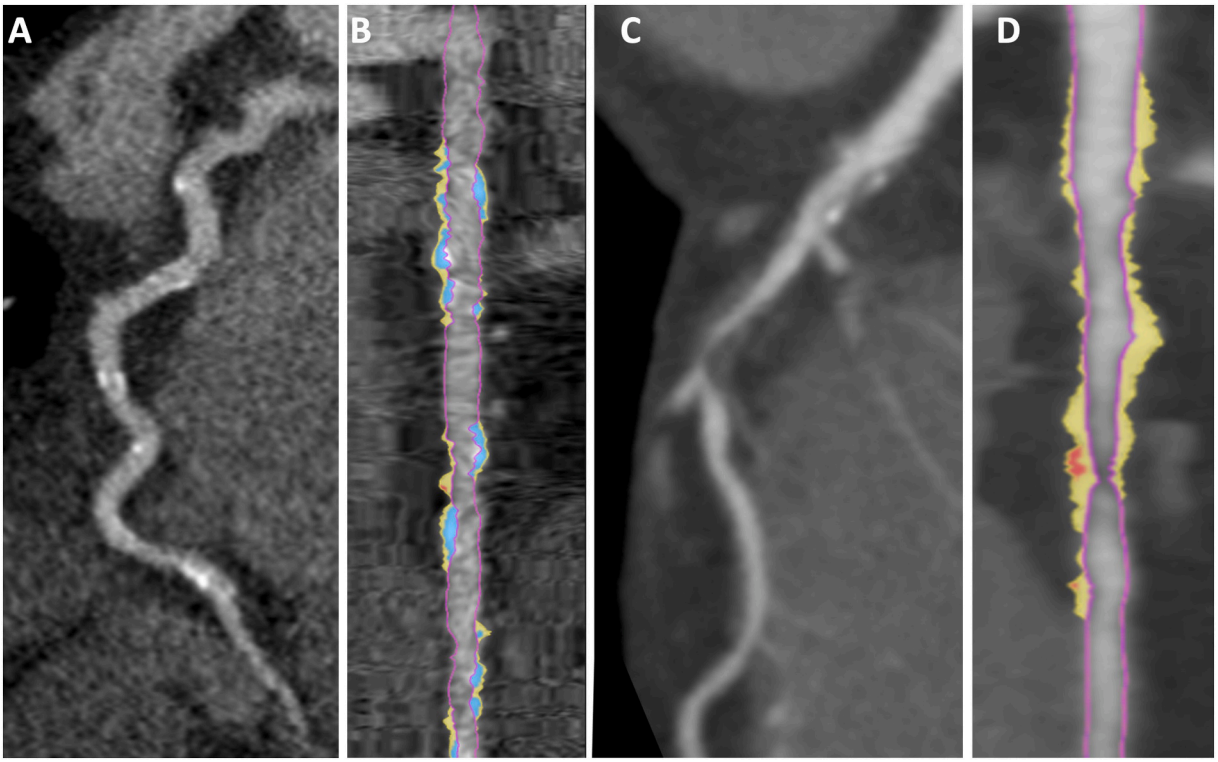

Fig. 2. Comparison of performance in two scans of differing image quality secondary to BMI differences. CCTA of a 53-year-old woman with a BMI of 34 demonstrates increased noise and low signal-to-noise ratio. Curved multiplanar reformat (A) depicts scattered nonobstructive plaques. AI-QCT analysis (B) depicts scattered mixed plaques and a 38% stenosis in the mid vessel; QCA depicted a 44% stenosis in this location. CCTA on a 62-year-old male with BMI 25 has significantly improved overall IQ and SNR (C). A 76% stenosis was depicted on AI-QCT, which corresponded to a 70% stenosis determined on QCA.

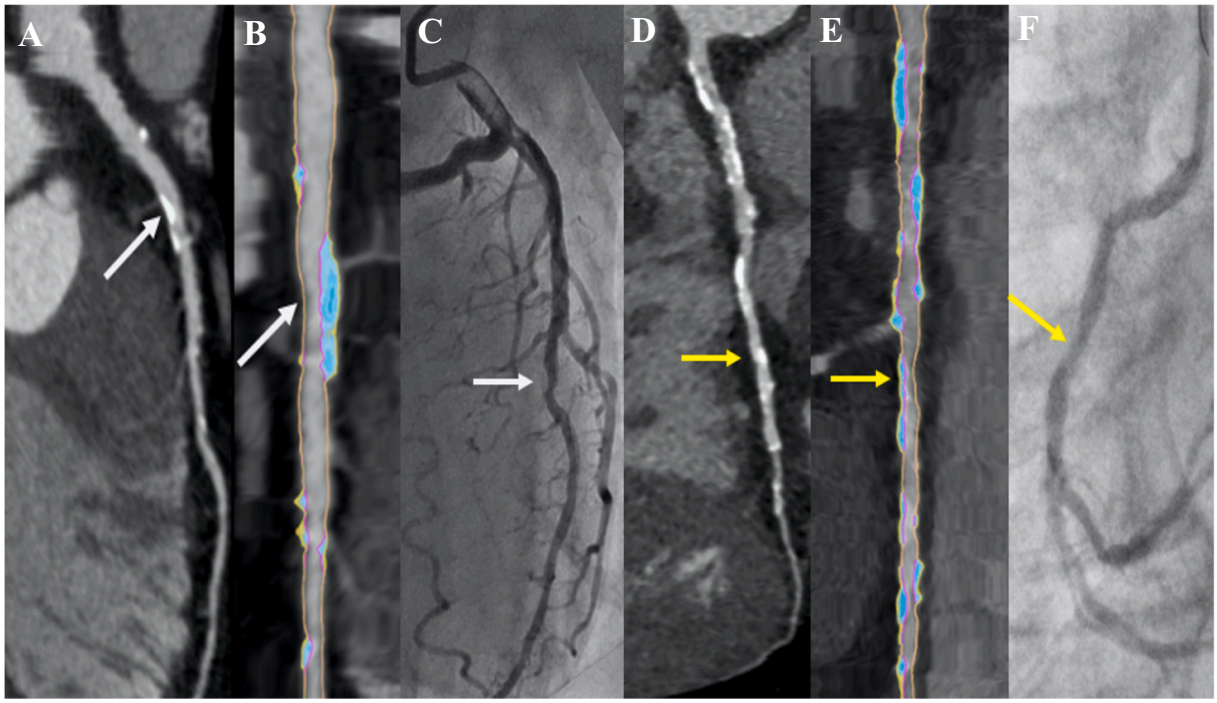

Fig. 3. Image quality secondary to iodine concentration differences with conventional coronary angiography correlation. CCTA on a 57 year old man using iodine with a concentration of 400 mg iodine per mL demonstrates high intra-arterial attenuation (480 HU) (A). AI-QCT (B) depicts a 50% stenosis in the mid LAD (arrow) which as determined to be 56% on quantitative coronary angiography (QCA) (arrow, C). CCTA on a 65 year old woman using iodine with a concentration of 320 mg iodine per mL demonstrates decreased intra-arterial attenuation (210 HU) (D). A 46% stenosis was depicted on AI QCT (arrow S), which corresponded to a 45% stenosis on QCA (arrow, E).

3.4. AI diagnostic measurements by scanning parameters at the level of the vessel territory

AI sensitivity, specificity, and accuracy measurements for detecting moderate stenosis at the level of the vessel territory, and per patient, are listed for each of the tested scanning parameters in Table 3. Data indicate that there were significant differences in sensitivity for detecting 50% stenosis based on contrast type (iso-osmolar 70.0% vs non iso-osmolar 92.1% $p = 0.0345$) and iodine concentration (<350 mg/ml 70.0%, 350-369 mg/ml 90.0%, 370–400 mg/ml 90.0%, >400 mg/ml 95.2%; $p = 0.0287$). There was no significant difference in the specificity or accuracy which remained comparable across both iodine concentrations and contrast types. There were no significant differences observed in diagnostic performance measurements for any other scanning parameters.

4. Discussion

This study evaluated the effect of CCTA scanning parameters on the performance of an FDA-cleared AI-enabled software capable of identifying and quantifying coronary stenoses and found that on a per-patient basis the software's sensitivity, specificity and accuracy for identifying lesions with ≥50% stenosis were unaffected by scanner type, gating technique, contrast features, radiation features, mode of image reconstruction or patients' clinical features at time of scan.

The natural variability amongst readers, the sheer volume of data as well as the time expenditure required for each read provide a foundation for the introduction of AI guided CCTA into the field of cardiac imaging.[10] To test the software's performance for stenosis identification and for plaque characterization, the CLARIFY trials compared the AI software against three gold standards, expert readers, QCA and FFR and showed AI performed strongly for stenosis identification and better than expert readers for plaque morphology.[10,11] This raises the question of whether accuracy and performance favors AI in addition to improving read expediency and data processing. Further studies are currently underway to evaluate this AI software's capability for plaque quantification and characterization against intravascular ultrasound and optical coherence tomography. However, based on current data, there is a strong basis for the use of AI for the identification or exclusion of moderate to severe stenoses given high performance against QCA, experts, and FFR.

As AI becomes more widely accepted in CCTA analysis, it becomes necessary to test its performance across a variety of scanning parameters as widespread use will require it to perform well across all parameter variants. But additionally, the functional and anatomical variability that necessitates adjustments in scanning parameters further reinforces the importance of high AI performance across a multitude of different settings. To date, AI has been used to minimize motion artifact in circumstances where patients are nonresponsive to beta blockers,[16] and to optimize phase selection when patients have abnormal heart rhythms.[17–19] While these programs paved the way for AI use for optimization of the imaging process, the AI software discussed in this study attacks the problem of interpretation itself, not just image optimization. Uniquely, this software was designed to automatically identify and calculate stenoses based on a series of algorithms that segment the coronary tree, identify a midline around which perpendicular slices are compared to identify the beginning, end and maximum point of stenosis in a lesion. The program subsequently employs deep learning to enhance its performance as it is exposed to more vessels. This is the first study to analyze the application of this AI program for stenosis identification across scanning parameters and supports that the software's performance is on par with the performance of QCA, an invasive gold standard for stenosis identification.[11]

CCTA images are generated using a variety of different scanning parameter combinations purposefully chosen by the CT technologist to optimize image quality while minimizing radiation exposure. While

Table 3
AI diagnostic performance by scanning parameter at the level of the vessel territory.

Subgroup	Sensitivity	Specificity	Accuracy
Scanner vendor			
GE	86.1% (37/43)	87.4% (104/119)	87.0% (141/162)
Philips	100% (6/6)	77.8% (7/9)	86.7% (13/15)
Siemens	92.2% (95/103)	84.0% (241/287)	86.2% (336/390)
Toshiba	92.0% (103/112)	81.3% (187/230)	84.8% (290/342)
	0.6239	0.6473	0.8013
Scanner model			
Toshiba – Aquilion One	92.0% (103/112)	81.3% (187/230)	84.8% (290/342)
GE-VCT Light Speed 64	86.1% (37/43)	86.9% (93/107)	86.7% (130/150)
Siemens Dual Source Definition	96.9% (31/32)	83.5% (96/115)	86.4% (127/147)
All others	92.5% (49/53)	87.5% (98/112)	89.1% (147/165)
	0.3414	0.4776	0.6559
Single source vs dual source			
SS	91.0% (202/222)	83.5% (416/498)	85.8% (618/720)
DS	92.9% (39/42)	83.7% (123/147)	85.7% (162/189)
	0.6779	0.8815	0.9693
Average heart rate during CT			
≤70 bpm	90.9% (200/220)	83.7% (436/521)	85.8% (636/741)
>70 bpm	96.9% (31/32)	82.3% (65/79)	86.4% (96/111)
	0.3036	0.8878	0.8863
≤75 bpm	92.9% (13/14)	83.3% (464/557)	85.8% (682/795)
>75 bpm	91.6% (218/238)	86.1% (37/43)	87.7% (50/57)
	0.8865	0.6119	0.7284
≤70	90.9% (200/220)	83.7% (436/521)	85.8% (636/741)
71–80	100% (25/25)	80.7% (50/62)	86.2% (75/87)
>80	85.7% (6/7)	88.2% (15/17)	87.5% (21/24)
	0.6420	0.9718	0.8392
Beta blocker IV			
Yes	91.3% (42/46)	81.1% (60/74)	85.0% (102/120)
No	91.3% (199/218)	83.9% (479/571)	85.9% (678/789)
	0.9910	0.5413	0.8010
Nitroglycerin dose			
None	91.9% (57/62)	83.4% (181/217)	85.3% (238/279)
Low (0.1–0.4 mg)	89.7% (61/68)	80.4% (131/163)	83.1% (192/231)
High (>0.4 mg)	91.8% (123/134)	85.7% (227/265)	87.7% (350/399)
	0.9915	0.4926	0.3450
None	91.9% (57/62)	83.4% (181/217)	85.3% (238/279)
Some	91.1% (184/202)	83.6% (358/428)	86.0% (542/630)
	0.7914	0.9938	0.7855
Bolus tracker or test bolus			
BT	92.4% (146/158)	81.5% (287/352)	84.9% (433/510)
TB	89.6% (95/106)	86.2% (250/290)	87.1% (345/396)
	0.4569	0.1492	0.3681
Gating technique			
Prospective/sequential/single beat	87.9% (102/116)	83.0% (195/235)	84.6% (297/351)
Retrospective helical			

(continued on next page)

Table 3 (*continued*)

Subgroup	Sensitivity	Specificity	Accuracy
	93.9% (139/148)	84.0% (342/407)	86.7% (481/555)
	0.0938	0.7001	0.4257
Contrast agent			
Visipaque	70.0% (7/10)	87.5% (28/32)	83.3% (35/42)
All others	92.1% (234/254)	83.4% (511/613)	85.9% (745/867)
	0.0345	0.5624	0.6777
Concentration mg iodine per mL			
Q1: <350	70% (7/10)	88.6% (31/35)	84.4% (38/45)
Q2: 350–369	90% (45/50)	85.3% (139/163)	86.4% (184/213)
Q3: 370–400	90.0% (90/100)	79.8% (186/233)	82.9% (276/333)
Q4: >400	95.2% (99/104)	85.8% (181/211)	88.9% (280/315)
	0.0287	0.9920	0.3223
Contrast injection rate (*cc/sec*)			
<5	88.7% (55/62)	82.4% (117/142)	84.3% (172/204)
5	91.7% (143/156)	85.9% (340/396)	87.5% (483/552)
>5	93.5% (43/46)	76.2% (77/101)	81.6% (120/147)
	0.3456	0.4741	0.6803
Contrast volume- *mg/kg body weight*			
Q1: <333.4	87.5% (49/56)	84.3% (145/172)	85.1% (194/228)
Q2: 333.4–408.2	90.8% (59/65)	80.0% (128/160)	83.1% (187/225)
Q3: 408.3–504.5	93.3% (70/75)	84.7% (127/150)	87.6% (197/225)
Q4: >504.5	92.6% (63/68)	85.6% (137/160)	87.7% (200/228)
	0.2671	0.5518	0.2633
Tube voltage			
≤80 kV	91.7% (11/12)	90.5% (38/42)	90.7% (49/54)
100 kV	88.6% (101/114)	80.9% (182/225)	83.5% (283/339)
120 kV	93.6% (117/125)	84.7% (298/352)	87.0% (415/477)
	0.2257	0.7881	0.6652
Dose length product (*mGy*cm*)			
Q1: <200.5	87.8% (42/46)	84.5% (125/148)	85.6% (190/222)
Q2: 200.5–365	91.8% (40/42)	88.2% (142/161)	89.2% (198/222)
Q3: 366–600.2	95.1% (42/43)	77.0% (124/161)	82.0% (182/222)
Q4: >600.2	90.9% (41/44)	84.6% (137/162)	86.4% (197/228)
	0.4324	0.3295	0.6740
BMI			
<30	91.6% (219/239)	83.9% (459/547)	86.3% (678/786)
≥30	88.0% (22/25)	81.6% (80/98)	82.9% (102/123)
	0.6232	0.5686	0.3194
Iterative reconstruction			
FBP	86.1% (37/43)	86.9% (93/107)	86.7% (130/150)
IR	92.3% (204/221)	82.9% (446/538)	85.6% (650/759)
	0.2073	0.4985	0.7591

various societal guidelines recommend specific techniques, investigators in the PROTECT VI (Prospective Multicenter Registry On RadiaTion Dose Estimates Of Cardiac CT AngIOgraphy IN Daily Practice in 2017) found that the protocols varied widely and that recommended techniques were not routinely adhered to.[20] Likely this was a function of the added necessity and complexity of adjusting parameters based on the clinical characteristics of patients at the time of scan.[21] In routinely performed clinical CCTA exams, selected scanning protocol parameters are selected based on patient requirements to produce diagnostically readable, though sometimes varied appearing images.

For CCTA, the gating technique has one of the greatest impacts on image appearance, diagnostic quality and radiation dose. Prospective gating is commonly used with lower heart rates. This technique minimizes radiation exposure by using a "step-and-shoot" approach of limited exposure during a small part of the cardiac cycle, usually diastole. The alternative is to continuously scan throughout the cardiac cycle, known as known as retrospective helical gating.[22] Prospective gating has been shown to have higher image quality scores than retrospective gating,[23] however, these results, and others from similar studies were dependent on patient specific variables including low and consistent heart rates.[21,24–26] Despite the potential for significant image quality differences between the techniques, we did not find that the gating technique affected diagnostic performance of the algorithm.

The image reconstruction techniques are known to affect image quality. Filtered back projection (FBP) has been the standard reconstruction algorithm since the invention of CT 50 years ago but has been known to produce images with greater noise than more recent techniques.[27] Iterative reconstruction (IR) is a newer and more computationally intense method which can typically produce images of better quality at lower radiation dose than FBP.[28,29] However, the additional filters used in IR scan generation can sharpen the appearance of a structure's edges which may result in loss of fine detail.[28] Consistently, at low radiation doses the Agatston score calculated from a calcium scoring CT based on IR generated images could vary by up to 15% from those calculated based on images using FBP.[30] As with gating techniques, we did not find any performance differences for the algorithm based on the reconstruction technique.

While our overall data show that there are no significant differences in AI performance compared to QCA across the scan parameters tested, there are a few caveats regarding iodine concentration, scanner model and scanner vendor that require further discussion. With regard to differences in iodine concentrations, it is important to recognize that the contrast type, its concentration of iodine, and injection rates all contribute to lumen enhancement. While high iodine concentrations increase vessel attenuation, they also increase patient heart rate, introducing potential motion artifacts into the image[31] or obscure the distinction between calcified and non-calcified plaque.[32,33] Iso-osmolar contrasts are consequently preferable but require higher flow rates at injection to achieve similar levels of vessel attenuation as dyes containing higher iodine concentrations.[31,34] While our findings indicate that AI was less sensitive to stenosis on a per vessel basis with Iodixanol (Visipaque) use, it is notable that the patients who received this dye were injected at a non-standard flow rate of 2–3 mL/s, well below the standard practice guidelines of 4–6 mL/s, likely resulting in low vessel attenuation. Additionally, the patient level specificity across scanner model and vendor were equivocal, likely due to low power of our cohort. However, overall, these data strongly support the use of AI guided CCTA based on a strong performance against a QCA gold standard.

This study has limitations. The present study was a post-hoc analysis of the CREDENCE trial and, while it is unexpected that significant bias would be introduced in a retrospective evaluation leveraging blinded core laboratory readers, it nevertheless emphasizes the absence of a prospective clinical trial that should be performed in the future. Further, this study evaluated the AI-based evaluation for measures of stenosis severity, rather than for plaque volume, composition, vascular remodeling and other important CAD metrics. Also, ground truth in this

present study was core-lab interpreted QCA for any stenosis >30%, in keeping with prior multicenter studies employing QCA. Because of this, we are not able report the diagnostic performance of the AI-based evaluation for the presence of stenosis lower than this range. Stenoses in this range have been historically considered inconsequential by QCA, although newer data suggest a prognostic significance to these "mild" lesions that may nevertheless possess high-risk atherosclerotic characteristics.

5. Conclusion

AI -QCT can identify moderate to high grade stenoses with high sensitivity, specificity and accuracy compared to QCA, the invasive gold standard. Furthermore, the diagnostic performance measurements of AI are unaffected by CCTA scanner, scan technique, radiation dose, patient preparation, contrast, and patient parameters.

Declaration of competing interest

Equity Interest Cleerly, Inc.: ADC, JPE, HM; Employee Cleerly, JPE, RSJ, TRC.

Appendix A. Inclusion and exclusion criteria

Inclusion criteria

1. Age >18 years
2. Scheduled to undergo clinically indicated non-emergent invasive coronary angiography

Exclusion criteria

1. Known CAD before index testing (myocardial infarction, percutaneous coronary intervention, or coronary artery bypass graft surgery)
2. Hemodynamic instability
3. Inability to provide written informed consent
4. Concomitant participation in another clinical trial in which subject is subject to investigational drug or device
5. Pregnant state
6. Contraindication to iodinated contrast due to prior near-fatal anaphylactic reaction (laryngospasm, bronchospasm, cardiorespiratory collapse, or equivalent)
7. Serum creatinine ≥1.7 mg/dl or Glomerular Filtration Rate <30 ml/min
8. Baseline irregular heart rhythm (e.g., atrial fibrillation, etc.)
9. Heart rate ≥100 beats per minute
10. Systolic blood pressure ≤90 mmHg
11. Contraindications to β blockers or nitroglycerin or adenosine
12. BMI >40 kg/m2

Appendix B. Participating sites and enrolling investigators

Investigator: Erick Avelar, MD
Oconee Heart and Vascular Center at St Mary's Hospital
Athens, GA, USA
Investigator: Hyuk-Jae Chang, MD PhD3
Severance Cardiovascular Hospital and Severance Biomedical Science Institute, Yonsei University College of Medicine, Yonsei University Health System Seoul, South Korea
Investigator: Jung Hyun Choi, MD PhD
Pusan National University Hospital Busan, South Korea
Investigator: Jason Cole, MD
Mobile Cardiology Associates Mobile, Alabama, USA
Investigator: Joon-Hyung Doh, MD
Inje University Ilsan Paik Hospital Goyang, South Korea
Investigator: Andrejs Erglis, MD
Pauls Stradins Clinical University Hospital Riga, Latvia
Investigator: Alessia Gimelli, MD, Dante Chiappino, MD
Fondazione Toscana Gabriele Monasterio Pisa, Italy
Investigator: Ae-Young Her, MD
Kang Won National University Hospital Chuncheon, South Korea
Investigator: James J. Jang, MD
Kaiser Permanente Hospital San Jose, CA, USA
Investigator: Muhammad Akram Khan, MD, Venkaa Chilakapati, MD, Ahmed Ladak, MD, Irfan Ullah, MD
Cardiac Center of Texas McKinney, Texas, USA
Investigators: Paul Knaapen, MD, PhD
Amsterdam University Medical Center VU University Medical Center Amsterdam, the Netherlands
Investigator: Bon-Kwon Koo, MD PhD
Seoul National University Hospital Seoul, South Korea
Investigator: Bin Lu, MD
State Key Laboratory of Cardiovascular Disease, Fuwai Hospital Beijing, China
Investigator: Atizazul Mansoor, MD
Pinnacle Health Cardiovascular Institute Harrisburg, PA, USA
Investigator: Faisal Nabi, MD
Houston Methodist Hospital Houston, Texas, USA
Investigators: Ryo Nakazato, MD, Hiroyumi Niinuma, MD
St. Luke's International Hospital Tokyo, Japan
Investigator: Chang-Wook Nam, MD PhD
Keimyung University Dongsan Hospital Daegu, South Korea
Investigator: Hyung-Bok Park, MD
International St. Mary's Hospital Catholic Kwandong University College of Medicine Incheon, South Korea
Investigator: Michael Ridner, MD
Heart Center Research, LLC Huntsville, Alabama, USA
Investigator: Chris Rowan, MD
Renown Heart and Vascular Institute Reno, NV, USA
Investigator: U. Joseph Schoepf, MD, Daniel Sternberg, MD
Medical University of South Carolina Charleston, SC, USA
Investigator: Sang-Hoon Shin, MD
National Health Insurance Service Ilsan Hospital Goyang, South Korea
Investigator: Randall C. Thompson, MD
St. Luke's Mid America Heart Institute Kansas City, MO, USA

References

1. Miller JM, et al. Diagnostic performance of coronary angiography by 64-row CT. N Engl J Med 2008;359(22):2324–36.
2. Budoff MJ, et al. Diagnostic performance of 64-multidetector row coronary computed tomographic angiography for evaluation of coronary artery stenosis in individuals without known coronary artery disease: results from the prospective multicenter ACCURACY (Assessment by coronary computed tomographic angiography of individuals undergoing invasive coronary Angiography) trial. J Am Coll Cardiol 2008;52(21):1724–32.
3. Min JK, et al. Prognostic value of multidetector coronary computed tomographic angiography for prediction of all-cause mortality. J Am Coll Cardiol 2007;50(12):1161–70.
4. Hadamitzky M, et al. Prognostic value of coronary computed tomographic angiography for prediction of cardiac events in patients with suspected coronary artery disease. JACC Cardiovasc Imaging 2009;2(4):404–11.
5. Chang HJ, et al. Selective referral using CCTA versus direct referral for individuals referred to invasive coronary angiography for suspected CAD: a randomized, controlled, open-label trial. JACC Cardiovasc Imaging 2019;12(7 Pt 2):1303–12.
6. Investigators S-H, et al. Coronary CT angiography and 5-year risk of myocardial infarction. N Engl J Med 2018;379(10):924–33.
7. Motwani M, et al. Machine learning for prediction of all-cause mortality in patients with suspected coronary artery disease: a 5-year multicentre prospective registry analysis. Eur Heart J 2017;38(7):500–7.
8. van Rosendael AR, et al. Maximization of the usage of coronary CTA derived plaque information using a machine learning based algorithm to improve risk stratification; insights from the CONFIRM registry. J Cardiovasc Comput Tomogr 2018;12(3):204–9.
9. Ambale-Venkatesh B, et al. Cardiovascular event prediction by machine learning: the multi-ethnic study of atherosclerosis. Circ Res 2017;121(9):1092–101.

10. Choi AD, et al. CT EvaLuation by ARtificial Intelligence For Atherosclerosis, Stenosis and Vascular MorphologY (CLARIFY): a multi-center, international study. J Cardiovasc Comput Tomogr 2021;15(6):470–6.
11. Griffin WF, et al. AI evaluation of coronary stenosis on CT coronary angiography, comparison with quantitative coronary angiography and fractional flow reserve; a CREDENCE trial sub-study. J Am Coll Cardiol Img 2022. https://doi.org/10.1016/j.jcmg.2021.10.020.
12. Rizvi A, et al. Rationale and design of the CREDENCE trial: computed TomogRaphic evaluation of atherosclerotic DEtermiNants of myocardial IsChEmia. BMC Cardiovasc Disord 2016;16(1):190.
13. Stuijfzand WJ, et al. Stress myocardial perfusion imaging vs coronary computed tomographic angiography for diagnosis of invasive vessel-specific coronary physiology: predictive modeling results from the computed tomographic evaluation of atherosclerotic determinants of myocardial ischemia (CREDENCE) trial. JAMA Cardiol 2020;5(12):1338–48.
14. Leipsic J, et al. SCCT guidelines for the interpretation and reporting of coronary CT angiography: a report of the Society of Cardiovascular Computed Tomography Guidelines Committee. J Cardiovasc Comput Tomogr 2014;8(5):342–58.
15. United States Food and Drug Administration. Cleerly Labs 510 (k) premarket notification. 2019. https://www.accessdata.fda.gov/cdrh_docs/pdf19/K190868.pdf.
16. Fuchs TA, et al. Impact of a new motion-correction algorithm on image quality of low-dose coronary CT angiography in patients with insufficient heart rate control. Acad Radiol 2014;21(3):312–7.
17. Stassi D, et al. Automated selection of the optimal cardiac phase for single-beat coronary CT angiography reconstruction. Med Phys 2016;43(1):324.
18. Oda S, et al. A low tube voltage technique reduces the radiation dose at retrospective ECG-gated cardiac computed tomography for anatomical and functional analyses. Acad Radiol 2011;18(8):991–9.
19. Lee AM, et al. Coronary computed tomography angiography during arrhythmia: radiation dose reduction with prospectively ECG-triggered axial and retrospectively ECG-gated helical 128-slice dual-source CT. J Cardiovasc Comput Tomogr 2012;6(3):172–183 e2.
20. Stocker TJ, et al. Application of low tube potentials in CCTA: results from the PROTECTION VI study. JACC Cardiovasc Imaging 2020;13(2 Pt 1):425–34.
21. Husmann L, et al. Body physique and heart rate variability determine the occurrence of stair-step artefacts in 64-slice CT coronary angiography with prospective ECG-triggering. Eur Radiol 2009;19(7):1698–703.
22. Earls JP. How to use a prospective gated technique for cardiac CT. J Cardiovasc Comput Tomogr 2009;3(1):45–51.
23. Earls JP, et al. Prospectively gated transverse coronary CT angiography versus retrospectively gated helical technique: improved image quality and reduced radiation dose. Radiology 2008;246(3):742–53.
24. Stolzmann P, et al. Dual-source CT in step-and-shoot mode: noninvasive coronary angiography with low radiation dose. Radiology 2008;249(1):71–80.
25. Muenzel D, et al. Step and shoot coronary CT angiography using 256-slice CT: effect of heart rate and heart rate variability on image quality. Eur Radiol 2011;21(11):2277–84.
26. Yang L, et al. 64-MDCT coronary angiography of patients with atrial fibrillation: influence of heart rate on image quality and efficacy in evaluation of coronary artery disease. Am J Roentgenol 2009;193(3):795–801.
27. Schofield R, et al. Image reconstruction: part 1 - understanding filtered back projection, noise and image acquisition. J Cardiovasc Comput Tomogr 2020;14(3):219–25.
28. Tayal U, et al. Image reconstruction in cardiovascular CT: part 2 - iterative reconstruction; potential and pitfalls. J Cardiovasc Comput Tomogr 2019;13(3):3–10.
29. Yin WH, et al. Iterative reconstruction to preserve image quality and diagnostic accuracy at reduced radiation dose in coronary CT angiography: an intraindividual comparison. JACC Cardiovasc Imaging 2013;6(12):1239–49.
30. den Harder AM, et al. Submillisievert coronary calcium quantification using model-based iterative reconstruction: a within-patient analysis. Eur J Radiol 2016;85(11):2152–9.
31. Honoris L, et al. Comparison of contrast enhancement, image quality and tolerability in coronary CT angiography using 4 contrast agents: a prospective randomized trial. Int J Cardiol 2015;186:126–8.
32. Cademartiri F, et al. Intravenous contrast material administration at helical 16-detector row CT coronary angiography: effect of iodine concentration on vascular attenuation. Radiology 2005;236(2):661–5.
33. Maffei E, et al. Plaque imaging with CT coronary angiography: effect of intravascular attenuation on plaque type classification. World J Radiol 2012;4(6):265–72.
34. Kim T, et al. Effects of injection rates of contrast material on arterial phase hepatic CT. Am J Roentgenol 1998;171(2):429–32.